CrystEngComm

PAPER

View Article Online
View Journal | View Issue

Cite this: *CrystEngComm*, 2018, **20**, 1232

Syntheses of copper–iodine cluster-based frameworks for photocatalytic degradation of methylene blue†

Juan Liu,[a] Yu-Huan Tang,[ab] Fei Wang *[a] and Jian Zhang *[a]

Received 20th December 2017,
Accepted 18th January 2018

DOI: 10.1039/c7ce02192e

rsc.li/crystengcomm

Two new copper–iodine cluster-based frameworks, namely, $\{Cu_4I_4[Cu(5\text{-eatz})_2]_2\}_n$ (**1**; 5-eatzH = (1*S*)-1-(5-tetrazolyl)ethylamine) and $\{Cu_4I_4Cu(5\text{-eatz})_2\}_n$ (**2**), are synthesized. For comparison purposes, the compound $\{2[N(CH_3)_4]^+\cdot Cu_{12}I_{12}[Cu^I(5\text{-eatz})_2]_2\}_n$ (**3**) reported by us is also included. These compounds have similar porphyrin-like $Cu(5\text{-eatz})_2$ units but different Cu–I sub-structures, for example, the discrete Cu_4I_4 unit in **1**, the 1D Cu–I graphene-like nanoribbon in **2** and the 3D Cu–I framework in **3**, which can be obtained under tunable synthesis conditions. These structure features lead to the deep color appearance of crystals and strong adsorption in the visible light region. The diffuse reflectance spectra show that compounds **1** and **2** exhibit very low E_g values, which are equal to 1.18 eV for **1** and 1.12 eV for **2**. Interestingly, all of them exhibit excellent intrinsic photocatalytic activity to degrade methylene blue (MB) under visible light. **2** shows better photocatalytic performance than **1** and **3**, and can almost completely degrade MB in 300 minutes (with a degradation amount of 90%) without any sacrificial agents. Meanwhile, their photocatalytic activities are in the order **3** < **1** < **2**, which is opposite that of their E_g (**3** > **1** > **2**) values (E_g**3** = 1.49 eV). Remarkably, all of **1**, **2** and **3** can completely photodegrade the MB solution in 30 minutes in the presence of H_2O_2. The results demonstrate the potential application of copper–iodine cluster-based frameworks for the photocatalytic degradation of organic dyes.

Introduction

Efficient removal of organic pollutants from wastewater has become a hot research topic due to its ecological and environmental importance. Several physical and chemical methods such as adsorption, membrane separation and photocatalysis on semiconductor catalysts (such as TiO_2) have been developed to remove organic pollutants.[1–4] However, physical methods often suffer from high costs and low efficiency. For the chemical methods, the catalysts are usually difficult to recycle, easy to aggregate, less efficient in solar energy conversion and may generate secondary pollutants. Thus, exploring new highly efficient visible light-driven photocatalysts has been one of the most attractive topics to address the above problem.

Metal–organic frameworks (MOFs) or porous coordination polymers (PCPs) have attracted great attention due to their feasibly tailored structures and potential applications in gas adsorption/separation,[5–11] catalysis,[12–15] and so on. Recently, MOFs have been reported as a new kind of photocatalyst for the degradation of organic pollutants in water under UV/visible/UV-visible light.[16–20] Theoretically, it is easy to construct MOFs with a tunable structure to absorb light for the photocatalytic degradation of specific organic pollutants. Copper–iodine cluster-based MOFs have been widely researched recently because of their excellent photochemical and photophysical properties and potential applications in the areas of sensors and luminescent materials.[21–24] Most of them absorb in the wavelength range of visible light to exhibit different colors,[25–28] which makes them excellent candidates for photocatalytic applications. However, research on this field has rarely been reported.

In our former work, the copper–iodine cluster-based MOF $\{2[N(CH_3)_4]^+\cdot Cu_{12}I_{12}[Cu^I(5\text{-eatz})_2]_2\}_n$ (5-eatzH = (1*S*)-1-(5-tetrazolyl) ethylamine) has been proved to be a good photocatalytic catalyst to degrade organic pollutants.[25] It not only shows high efficiency in photocatalytic degradation but can also be recycled after several cycles. This result demonstrates that copper–iodine cluster-based MOFs may be potential photocatalysts.

Also, we found that the chiral tetrazolate derivative (5-eatzH) is easy to assemble with Cu ions into enantiopure

[a] *State Key Laboratory of Structural Chemistry, Fujian Institute of Research on the Structure of Matter, Chinese Academy of Sciences, Fuzhou, Fujian, 350002 P. R. China. E-mail: wangfei04@fjirsm.ac.cn, zhj@fjirsm.ac.cn*
[b] *University of Chinese Academy of Sciences, 100049 Beijing, P. R. China*

† Electronic supplementary information (ESI) available: IR, TG, PXRD and additional figures. CCDC 1554621 for **1** and 1554622 for **2**. CCDC 1554621–1554622. For ESI and crystallographic data in CIF or other electronic format see DOI: 10.1039/c7ce02192e

porphyrin-like Cu(5-eatz)$_2$ units, which possess *cis*- and *trans*-configurations (Scheme 1).[29–31] A series of multifunctional MOFs based on such Cu(5-eatz)$_2$ units were synthesized, which show excellent luminescence, enantioselective separation and dye degradation.[29]

In this work, we continue to combine Cu(5-eatz)$_2$ with copper–iodine clusters, and two new copper–iodine cluster-based MOFs, namely, $\{Cu_4I_4[Cu(5\text{-eatz})_2]_2\}_n$ (**1**) and $\{Cu_4I_4Cu(5\text{-eatz})_2\}_n$ (**2**), are synthesized. For comparison purposes, the compound $\{2[N(CH_3)_4]^+\cdot Cu_{12}I_{12}[Cu^I(5\text{-eatz})_2]_2\}_n$ (**3**) reported by us is also included. Interestingly, these compounds have similar Cu(5-eatz)$_2$ units but different Cu–I sub-structures. More importantly, they show intrinsic and remarkable photocatalytic activity to degrade methylene blue under visible light without any sacrificial agents. The results further prove that copper–iodine cluster-based MOFs are excellent candidates for the photocatalytic degradation of organic pollutants.

Experimental section

Materials and methods

Powder X-ray diffraction (PXRD) analyses were conducted using a MiniFlex II diffractometer with Cu Kα radiation (λ = 1.54056 Å), with a step size of 0.05°. Elemental analyses of C, H, and N were performed using a Vario MICRO EIII elemental analyzer. The IR spectra (KBr pellets) were recorded on a Magna 750 FTIR spectrophotometer. Thermogravimetric analyses (TGAs) were conducted on a NETZSCH STA-449C thermoanalyzer at a heating rate of 10 °C min^{-1} under a N_2 atmosphere. Solid state fluorescence properties were studied at room temperature with a HORIBA Jobin-Yvon FluoroMax-4 spectrometer.

Preparation of $\{Cu_4I_4[Cu(5\text{-eatz})_2]_2\}_n$ (1)

5-eatzH (0.15 mmol, 0.0175 g) is dissolved in 1 ml MeOH, and then CuI (0.15 mmol, 0.0281 g) in KI (1.352 g) aqueous solution (1.5 ml) was added to the former solution. The mixture was then stirred for 10 minutes and transferred into an oven at 120 °C for 12 hours; orange rod-like crystals were obtained and washed with KI aqueous solution, H_2O and EtOH. Anal. calc. for $C_{12}H_{16}N_{20}Cu_6I_4$ (M_w = 1329.35): C, 10.84; H, 1.21; N, 21.07%. Found: C, 11.02; H, 1.13; N, 21.35%. IR (KBr, cm^{-1}): 3435 (s), 3245 (s), 3210 (s), 3109 (s), 2969 (m), 2911 (m), 2861 (s), 2224 (s), 1615 (m), 1568 (s), 1498 (m), 1444 (w), 1417 (s), 1382 (w), 1354 (w), 1308 (w), 1207 (s), 1153 (s), 1114 (s), 1087 (s), 1044 (m), 1006 (m), 893 (m), 769 (s), 683 (m), 621 (m), 544 (m), 497 (w), 454 (m).

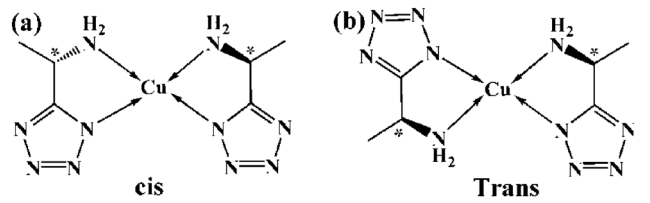

Scheme 1 The *cis*- (a) and *trans*- configurations (b) of the Cu(5-eatz)$_2$ unit.

Preparation of $\{Cu_4I_4Cu(5\text{-eatz})_2\}_n$ (2)

5-eatzH (0.15 mmol, 0.0175 g) and CuI (0.15 mmol, 0.0281 g) were added to H_2O and CH_3CN. The mixture was then stirred for 10 minutes and transferred into the oven at 120 °C for 12 hours; orange block crystals were obtained and washed with EtOH. Anal. calc. for $C_6H_5N_{10}Cu_5I_4$ (M_w = 1042.55): C, 6.91; H, 0.48; N, 13.44%. Found: C, 6.74; H, 0.52; N, 13.24%. IR (KBr, cm^{-1}): 3435 (s), 3245 (s), 3210 (s), 3109 (s), 2969 (m), 2911 (m), 2861 (s), 2224 (s), 1615 (m), 1568 (s), 1498 (m), 1444 (w), 1417 (s), 1382 (w), 1354 (w), 1308 (w), 1207 (s), 1153 (s), 1114 (s), 1087 (s), 1044 (m), 1006 (m), 893 (m), 769 (s), 683 (m), 621 (m), 544 (m), 497 (w), 454 (m).

Crystallography

The diffraction data for **1** and **2** were collected using an Oxford Xcalibur diffractometer equipped with graphite-monochromatized MoKα radiation (λ = 0.71073 Å) at 293(2) K. The structures were determined by direct methods and refined on F^2 full-matrix least-squares using the SHELXTL-2014 program package.

Photodegradation experiments

At room temperature, 0.0125 g crystals of **1**, **2** and **3** were added into 15 mL of 55 mgL^{-1} methylene blue aqueous solution. Then 30% H_2O_2 solution (40 μL) was injected into the above solution. Afterwards, the suspensions were stirred and exposed to a 300 W daylight lamp. To monitor the extent of reaction, reaction samples were prepared every 5 minutes until the solution becomes colourless. Generally, a 0.5 ml reaction solution was transferred and diluted to 3 mL. Then the diluted reaction solutions were filtered and their absorbances were measured using a UV-vis spectrophotometer (Lambda 35). To prove the stability of the catalyst, a four-cycle test was performed. After each cycle, the photocatalysts were separated, washed with ethanol, and dried at room temperature.

The photodegradation reactions of the MB aqueous solution catalysed by **1**, **2** and **3** without H_2O_2 were the same as above. Meanwhile, the photodegradation reaction of the MB aqueous solution catalysed by H_2O_2 was the same as above, except that **1** (**2** or **3**) was not added. To monitor the extent of reaction, reaction samples were prepared every 60 minutes. For a comparison of adsorption with photodegradation by **1** and **2**, MB adsorption in the dark was carried out using the same procedure as the photocatalytic experiments of **1** and **2** without H_2O_2 in the absence of light.

Results and discussion

Description of crystal structures

Crystal structure of $\{Cu_4I_4[Cu(5\text{-eatz})_2]_2\}_n$ (1). Compound **1** crystallizes in the monoclinic space group $P2_1$, and its asymmetric unit includes four Cu^I ions, four I$^-$ anions, two Cu^{II} ions and four 5-eatz ligands (Fig. 1a). Each Cu^{II} ion is chelated by two 5-eatz ligands to form the *trans*-Cu(5-eatz)$_2$ unit. All the Cu^I ions adopt the tetrahedral mode, and are

coordinated by I^- and N atoms from the 5-eatz ligands.[39,40] Each 5-eatz ligand coordinates to two Cu^I ions and chelates with one Cu^{II} ion *via* its four N atoms. All the Cu^I ions are linked by two μ_3-I^- anions to form a Cu_4I_2 unit, and another two I^- anions are pendent on both sides of the Cu_4I_2 unit to form the discrete Cu_4I_4 unit (Fig. 1a). Then each Cu_4I_4 unit is linked by four $Cu(5\text{-eatz})_2$ units, and each $Cu(5\text{-eatz})_2$ links two Cu_4I_4 units to generate a 2D layer (Fig. 1b). Such layers are parallel to each other and stack in the A-B-C mode. No obvious interactions are observed between the 2D layers. The mixed valence of the Cu ions is proven by the XPS pattern (Fig. S2†).

Crystal structure of $\{(Cu^I_4I_4)Cu^{II}(5\text{-eatz})_2\}_n$ (2)

Compound 2 also crystallizes in the monoclinic space group $P2_1$. The asymmetric unit of 2 contains four Cu^I ions, four I^- anions, one Cu^{II} ion and two 5-eatz ligands (Fig. 2a and S2†). Similar to 1, the Cu^{II} ion is chelated by two 5-eatz ligands to form the *trans*-$Cu(5\text{-eatz})_2$ unit. And all the Cu^I ions adopt the tetrahedral mode, and are also coordinated by I^- and N atoms from the 5-eatz ligands. However, unlike 1, each 5-eatz ligand in 2 coordinates to three Cu^I ions and chelates with one Cu^{II} ion *via* all of its N atoms.

The prominent structural feature of 2 is the presence of a 1D graphene-like $(CuI)_n$ nanoribbon (Fig. 2b). The Cu^I ions and I^- anions alternately link each other to form a 1D distorted zigzag chain along the *a*-axis. Then two adjacent zigzag $(CuI)_n$ chains link each other to generate such a 1D graphene-like $(CuI)_n$ nanoribbon *via* Cu–I bonds. This 1D graphene-like $(CuI)_n$ nanoribbon can also be considered as the repeat of Cu_4I_4 units (Fig. 2b). It should be noted that although the 1D ladder-like and 2D graphene-like SBUs based on Cu–halogen have been reported before,[32] to the best of our knowledge, such a 1D graphene-like $(CuI)_n$ nanoribbon is observed for the first time. Finally, such $(CuI)_n$ nanoribbons are linked by $Cu(5\text{-eatz})_2$ SBUs through Cu–N bonds into a 3D neutral framework (Fig. 2c).

The controllable synthesis of copper–iodine cluster-based metal–organic frameworks (MOFs) is of much interest. From the above structure analyses, we can find that all the compounds 1, 2 and 3 have $Cu(5\text{-eatz})_2$ units and Cu_4I_4-based units. The control of different synthetic conditions results in different Cu–I sub-structures (Fig. 3). As reported before, using 5-eatzH and CuI as the reactants in the presence of KI

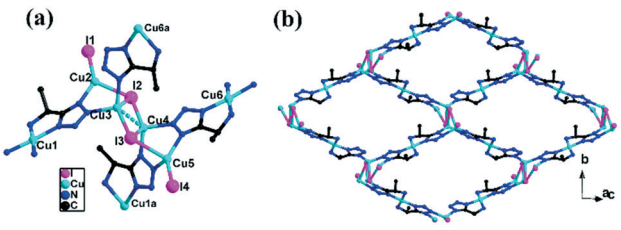

Fig. 1 (a) The coordination environment of compound 1; (b) the 2D layer of 1.

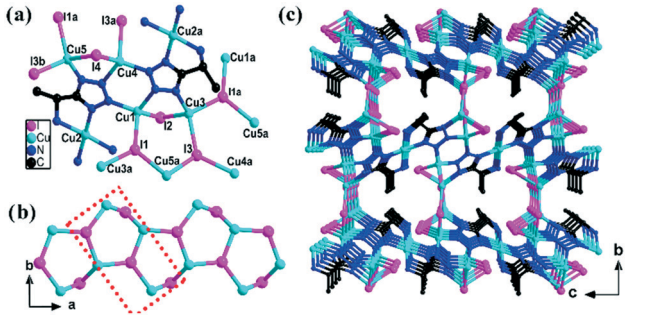

Fig. 2 (a) The coordination environment of 2, (b) the 1D $(CuI)_n$ nanoribbon in 2, and (c) the 3D framework of 2.

and $N(CH_3)_4^+$, the anionic compound 3 was obtained in which two kinds of Cu_4I_4 units linked each other to form a pure inorganic 3D framework. Meanwhile, the neutral 2D layer of 1 was synthesized under similar conditions without $N(CH_3)_4^+$ and discrete Cu_4I_4 units were observed. In the absence of KI and $N(CH_3)_4^+$, compound 2 was obtained and the Cu_4I_4 repeated units linked themselves to form the 1D nanoribbon. These structure features can further affect their photocatalytic activities, which are described in the following details.

Photocatalytic activities

Considering that compounds 1 and 2 are copper–iodine cluster compounds with a deep color, their diffuse reflectance spectra were studied (Fig. 4 and S5†). The spectra of these compounds show a broad range of absorption in the visible region from 400 nm to 900 nm with an absorption peak centered at around 520 nm. The spectra match well with their colors. According to the equation $\alpha h\nu^2 = K(h\nu - E_g)^{1/2}$ (where α is the absorption coefficient, $h\nu$ is the discrete photo energy, K is a constant, and E_g is the band gap energy), the extrapolated values (the straight lines to the x axis) of $h\nu$ at α =

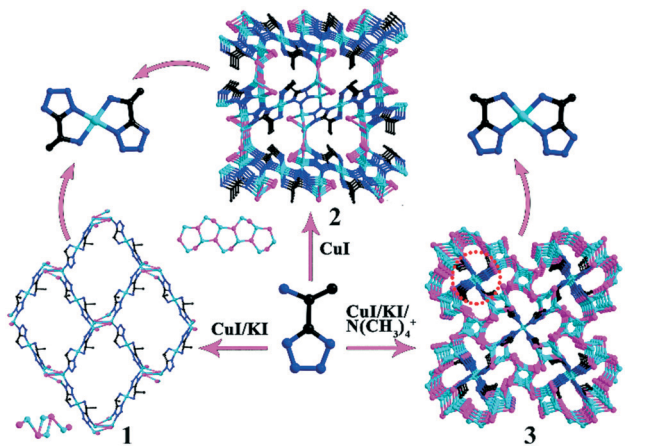

Fig. 3 The controllable synthesis of compounds 1–3: different synthetic conditions result in the discrete Cu_4I_4 unit in 1, the 1D Cu–I graphene-like nanoribbon in 2 and the 3D Cu–I framework in 3. These different Cu–I sub-structures further link the porphyrin-like $Cu(5\text{-eatz})_2$ units into different structures.

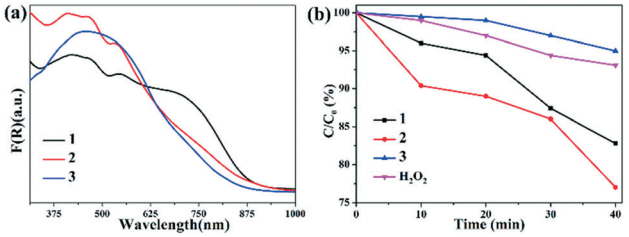

Fig. 4 (a) The solid state UV-vis reflectance spectra of compounds **1**, **2** and **3**, which show a broad range of absorption in the visible region from 400 nm to 900 nm; (b) the MB photodegradation of **1**, **2**, **3** and H_2O_2.

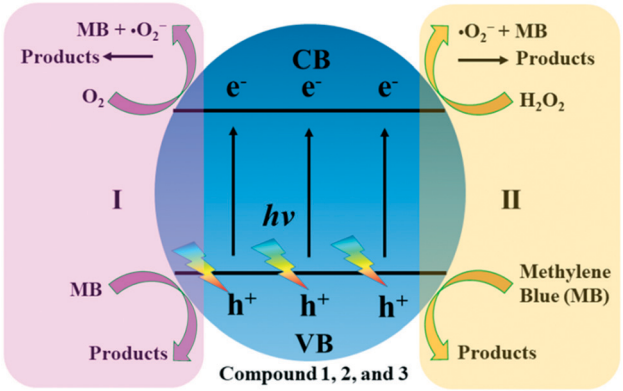

Fig. 5 (I) Possible mechanism of MB photodegradation over compounds **1**, **2** and **3** under visible light irradiation. (II) Possible mechanism of MB photodegradation over **1**, **2** and **3** in the presence of H_2O_2 under visible light irradiation.

0 give absorption edge energies (E_g) of 1.18 eV for **1** and 1.12 eV for **2** (Fig. S5†), which are lower than those of **3** (1.49 eV) and most MOF-based photocatalysts.[32]

To evaluate the photocatalytic activities of **1** and **2**, ethylene blue (MB) photodegradation under visible light illumination was performed. As shown in Fig. 4b, without any sacrificial agents, the concentration of methylene blue is reduced by 17% (for **1**) and 24% (for **2**) from 0 to 40 min, which is better than that for **3** (5%) under the same conditions (Fig. 4b and S6†). For easy comparison, the reaction kinetics of the MB degradation catalyzed by various photocatalysts (compounds **1**, **2** and **3**) were studied (Fig. S7†). The experimental data were fitted by a linear fitting model. The slopes, in proportion to the reaction rate constant, of the compounds are equal to −0.4453, −0.5448 and −0.1042, indicating that the reaction rate constants of these compounds are in the order **3** < **1** < **2**. Interestingly, both the degradation amount and reaction rate constant indicate that the photocatalytic activities of the compounds are in the order **3** < **1** < **2**, which is opposite that of their E_g (**3** > **1** > **2**) values. More importantly, compound **1** can almost completely photodegrade the MB solution in 300 minutes, with a photodegradation amount of 90% (Fig. S8 and S9†). Meanwhile, compound **2** shows a MB photodegradation amount of 50% at 300 minutes. At 360 minutes, the decrease in the concentration of the MB solution due to photodegradation by **1** and **2** is almost the same as that at 300 minutes. These results suggest that compounds **1** and **2** have higher intrinsic catalytic properties for methylene blue degradation than most reported MOFs (Table S2†).[32–38]

Furthermore, in the controlled photodegradation reactions catalysed by **1** and **2** in the presence of a small amount of additive, H_2O_2, the MB solution can be completely degraded in 30 minutes (Fig. S10†), which is similar to **3**, but much higher than most of the reported MOFs (Table S2†).[32–38] These results also illustrate that compounds **1**, **2** and **3** are excellent photocatalysts under visible light.

Accordingly, the reaction mechanism for MB photodegradation was discussed based on semiconductor theory. As shown in Fig. 5, path I accounts for the mechanism of MB photodegradation by compounds **1** and **2**. Path II shows the mechanism of MB photodegradation by compounds **1** and **2** in the presence of H_2O_2 additive. Firstly, the electrons (e) will be excited from the valence band (VB) to the conduction band (CB) when compounds **1** and **2** are illuminated by photons with energy equal to or greater than their band gaps, leaving holes (h^+) in the valence band (Fig. 5). The photoexcited holes (h^+) have a strong oxidant ability and can directly oxidize adsorbed organic molecules both in path I and path II.

Meanwhile, in path I, electrons can be trapped by molecular oxygen to form superoxide radicals, $^{\bullet}O_2^-$, which also possess a strong oxidant ability to decolorize the MB molecules, as shown in Fig. 5. In path II, the $^{\bullet}O_2^-$ radicals directly photoexcited from H_2O_2 also possess a strong oxidation ability and can react readily with surface adsorbed MB.

Conclusions

In summary, two copper–iodine cluster-based MOFs based on porphyrin-like $Cu(5\text{-eatz})_2$ units are controllably synthesized and fully studied here. These compounds show a deep color and a broad range of absorption in UV-vis light, which enables them to possess a superior ability in MB photodegradation. The possible MB degradation mechanism was systematically discussed, which can be explained by semiconductor theory. The results indicate that copper–iodine cluster-based MOFs are good candidates for the photocatalytic degradation of organic pollutants.

Conflicts of interest

There are no conflicts to declare.

Acknowledgements

This work is supported by the NSFC (21573236 and 21425102) and the Chunmiao Project of Haixi Institute of Chinese Academy of Sciences (CMZX-2015-001).

Notes and references

1 V. K. Gupta, I. Ali, T. A. Saleh, A. Nayak and S. Agarwal, *RSC Adv.*, 2012, 2, 6380–6388.

2 A. Mittal, J. Mittal, A. Malviya, D. Kaur and V. K. Gupta, *J. Colloid Interface Sci.*, 2010, **342**, 518–527.
3 A. Mittal, D. Kaur, A. Malviya, J. Mittal and V. K. Gupta, *J. Colloid Interface Sci.*, 2009, **337**, 345–354.
4 A. Mittal, J. Mittal, A. Malviya and V. K. Gupta, *J. Colloid Interface Sci.*, 2009, **340**, 16–26.
5 J. Yang, Y.-B. Zhang, Q. Liu, C. A. Trickett, E. Gutiérrez-Puebla, M. Á. Monge, H. Cong, A. Aldossary, H. Deng and O. M. Yaghi, *J. Am. Chem. Soc.*, 2017, **139**, 6448–6455.
6 C.-C. Liang, Z.-L. Shi, C.-T. He, J. Tang, H.-D. Zhou, H.-L. Zhou, Y. Lee and Y.-B. Zhang, *J. Am. Chem. Soc.*, 2017, **139**, 13300–13303.
7 D.-M. Chen, N.-N. Zhang, J.-Y. Tian, C.-S. Liu and M. Du, *J. Mater. Chem. A*, 2017, **5**, 4861–4867.
8 R.-B. Lin, S. Xiang, H. Xing, W. Zhou and B. Chen, DOI: 10.1016/j.ccr.2017.09.027.
9 L. Wang, Y. Ye, Z. Li, Q. Lin, J. Ouyang, L. Liu, Z. Zhang and S. Xiang, *Cryst. Growth Des.*, 2017, **17**, 2081–2089.
10 J. Duan, M. Higuchi, J. Zheng, S.-I. Noro, I. Y. Chang, K. Hyeon-Deuk, S. Mathew, S. Kusaka, E. Sivaniah, R. Matsuda, S. Sakaki and S. Kitagawa, *J. Am. Chem. Soc.*, 2017, **139**, 11576–11583.
11 J. Duan, W. Jin and S. Kitagawa, *Coord. Chem. Rev.*, 2017, **332**, 48–74.
12 X.-J. Hong, Q. Wei, Y.-P. Cai, B. Wu, H.-X. Feng, Y. Yu and R.-F. Dong, *ACS Appl. Mater. Interfaces*, 2017, **9**, 29374–29379.
13 J. Peng, H. Wang, D. H. Olson, Z. Li and J. Li, *Chem. Commun.*, 2017, **53**, 9332–9335.
14 D. Banerjee, S. K. Elsaidia and P. K. Thallapally, *J. Mater. Chem. A*, 2017, **5**, 16611–16615.
15 J. Ma, J. Guo, H. Wang, B. Li, T. Yang and B. Chen, *Inorg. Chem.*, 2017, **56**, 7145–7150.
16 Q. Yang, Q. Xu and H.-L. Jiang, *Chem. Soc. Rev.*, 2017, **46**, 4774–4808.
17 A. Dhakshinamoorthy, A. M. Asiri and H. Garcia, *ACS Catal.*, 2017, **7**, 2896–2919.
18 M. Mon, J. Ferrando-Soria, T. Grancha, F. R. Fortea-Pérez, J. Gascon, A. Leyva-Pérez, D. Armentano and E. Pardo, *J. Am. Chem. Soc.*, 2016, **138**, 7864–7867.
19 R. Saravana, M. M. Khan, V. K. Gupta, E. E. M. Vargas, F. Gracia, V. Narayanan and A. Stephen, *RSC Adv.*, 2015, **5**, 34645–34651.
20 S. Rajendran, M. M. Khan, F. Gracia, J. Qin, V. K. Gupta and S. Arumainathan, *Sci. Rep.*, 2016, **6**, 31641–31651.
21 C.-C. Wang, J.-R. Li, X.-L. Lv, Y.-Q. Zhang and G. Guo, *Energy Environ. Sci.*, 2014, **7**, 2831–2867.
22 M. C. Ortega-Liebana, J. L. Hueso, S. Ferdousi, R. Arenal, S. Irusta, K. L. Yeung and J. Santamaria, *Appl. Catal., B*, 2017, **218**, 68–79.
23 Y. Zhao, Y. Dong, F. Lu, C. Ju, L. Liu, J. Zhang, B. Zhang and Y. Feng, *J. Mater. Chem. A*, 2017, **5**, 15380–15389.
24 D. Wang, J. Albero, H. Garcia and Z. H. Li, *J. Catal.*, 2017, **349**, 156–162.
25 L.-X. Hu, M. Gao, T. Wen, Y. Kang and S. Chen, *Inorg. Chem.*, 2017, **56**, 6507–6511.
26 H. Park, E. Kwon, H. Chiang, H. Im, K. Y. Lee, J. Kim and T. H. Kim, *Inorg. Chem.*, 2017, **56**, 8287–8294.
27 B. Huitorel, H. E. Moll, M. Cordier, A. Fargues, A. Garcia, F. Massuyeau, C. Martineau-Corcos, T. Gacoin and S. Perruchas, *Inorg. Chem.*, 2017, **56**, 12379–12388.
28 Y.-L. Hou, R. W.-Y. Sun, X.-P. Zhou, J.-H. Wang and D. Li, *Chem. Commun.*, 2014, **50**, 2295–2297.
29 J. Liu, F. Wang, L.-Y. Liu and J. Zhang, *Inorg. Chem.*, 2016, **55**, 1358–1360.
30 J. Liu, F. Wang, Q.-R. Ding and J. Zhang, *Inorg. Chem.*, 2016, **55**, 12520–12522.
31 J. Liu, F. Wang and J. Zhang, *Cryst. Growth Des.*, 2017, **17**, 5393–5397.
32 R. Peng, M. Li and D. Li, *Coord. Chem. Rev.*, 2010, **254**, 1–18.
33 L. Ai, C. Zhang, L. Li and J. Jiang, *Appl. Catal., B*, 2014, **148**, 191–200.
34 H. Yang, X.-W. He, F. Wang, Y. Kang and J. Zhang, *J. Mater. Chem.*, 2012, **22**, 21849–21851.
35 X. Li, Y. Pi, L. Wu, Q. Xia, J. Wu, J. Li, Z. Li and J. Xiao, *Appl. Catal., B*, 2017, **202**, 653–663.
36 C.-F. Zhang, L.-G. Qiu, F. Ke, Y.-J. Zhu, Y.-P. Yuan, G.-S. Xu and X. Jiang, *J. Mater. Chem. A*, 2013, **1**, 14329–14334.
37 W.-T. Wu, L. Ma, F. Ke, F.-M. Peng, G.-S. Xu and Y.-H. Shen, *Dalton Trans.*, 2014, **43**, 3792–3798.
38 H.-P. Jing, C.-C. Wang, Y.-W. Zhang, P. Wang and R. Li, *RSC Adv.*, 2014, **4**, 54454–54462.
39 J.-R. Li, Q. Yu, E. C. Sañudo, Y. Tao and X.-H. Bu, *Chem. Commun.*, 2007, 2602–2604.
40 Y.-F. Yue, B.-W. Wang, E.-Q. Gao, C.-J. Fang, C. He and C.-H. Yan, *Chem. Commun.*, 2007, 2034–2036.

